Semiconducting Lithium

International Edition: DOI: 10.1002/anie.201608490
German Edition: DOI: 10.1002/ange.201608490

Quasimolecules in Compressed Lithium

Mao-sheng Miao, Roald Hoffmann,* Jorge Botana, Ivan I. Naumov, and Russell J. Hemley*

Abstract: *Under high pressure, some materials form electrides, with valence electrons separated from all atoms and occupying interstitial regions. This is often accompanied by semiconducting or insulating behavior. The interstitial quasiatoms (ISQ) that characterize some high pressure electrides have been postulated to show some of the chemical features of atoms, including the potential of forming covalent bonds. It is argued that in the observed high-pressure semiconducting Li phase (oC40, Aba2), an example of such quasimolecules is realized. The theoretical evaluation of electron density, electron localization function, Wannier orbitals, and bond indices forms the evidence for covalently bonded ISQ pairs in this material. The quasimolecule concept thus provides a simple chemical perspective on the unusual insulating behavior of such materials, complementing the physical picture previously presented where the global crystal symmetry of the system plays the major role.*

Electrides are materials in which some valence electrons are separated from all atoms and occupy interstitial regions, effectively forming anions with no centering nuclei nor core electrons.[1] Under high pressure, alkali metals such as Li and Na become semiconducting or insulating.[2,3] As they do so, they adopt structures containing sites that accommodate electrons, leading to the formation of high-pressure electrides (HPE).[4–6] Similar phenomena have also been predicted for Mg,[7] Al,[8] and several other materials.[9] The driving force for HPE formation may be attributed to the lack of core electrons in the interstitial sites, which causes the energies of the corresponding quantized orbitals to increase less significantly with pressure than normal atomic orbitals.[10] These empty sites enclosed by surrounding atoms and possessing quantized orbitals have been termed interstitial quasiatoms (ISQ); they may show some of the chemical features of atoms, including the potential of forming covalent bonds.[11]

Li has been found to become semiconducting at about 80 GPa in diamond anvil cell experiments.[2] The detailed structure of this new phase of Li was suggested by two computational studies that employed different crystal structure search methods.[5,6] The identified structure (oC40, *Aba*2 symmetry) is reasonably complex, containing 40 Li atoms in a base-centered orthorhombic cell (20 atoms in the primitive cell). This phase has a layered appearance with seemingly open areas (Figure 1a, a view along the *a* axis). We recalculated the atomic and electronic structures of this Li phase using PBE functional[12] and projector augmented-wave method (PAW)[13] as implemented in VASP program[14] (see the Supporting Information for details). The charge density distribution of *Aba*2 Li (Figure 1b) shows not only peaks at Li sites but also peaks at interstitial sites, revealing the positions of the ISQs. There are three symmetry-distinct sites for these, two of which we call collectively (for reasons to be specified) E^{II}, and one E^{I} (at Wyckoff positions 2*a* in the unit cell, coordinates given in the Supporting Information). In the original work on these phases, E^{II} was labeled M1 and M2, and E^{I} as M3.[5]

If Bader's quantum theory of atoms in molecules (QTAIM)[15] is applied to materials under compression, regions of high electron density off atoms may generate

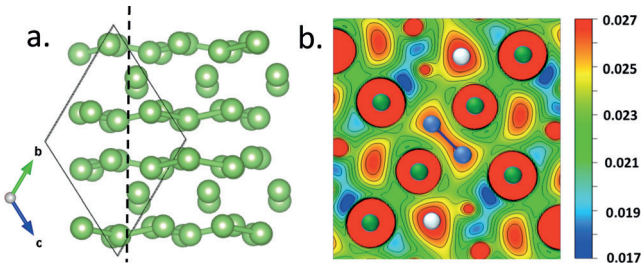

Figure 1. Calculated structural features of Li in *Aba*2, oC40 phase, including the ISQs, at 60 GPa. a) One view of the phase; the solid lines mark the primitive cell of 20 lithiums; b) one section of the total valence charge density (electrons bohr^{-3}) of *Aba*2 Li, in a plane perpendicular to the *b*–*c* plane, in Miller index plane (011), 1.2 units from origin. The plane is shown by a dashed line in (a). Green balls mark the Li nuclei, white and blue balls show the locations of the centers of E^{II} and E^{I}. The plane chosen in this cut contains the two E ISQs but not the Li atoms and other ISQs. The green and the white balls are only added to show that those high charge density areas stem from the Li atoms and the other ISQs, whose center in fact lie outside the plane chosen.

[*] Prof. M.-S. Miao, Dr. J. Botana
Department of Chemistry and Biochemistry
California State University, Northridge, CA 91330 (USA)
and
Beijing Computational Science Research Center
Beijing 10084 (P.R. China)
E-mail: mmiao@csun.edu
Prof. R. Hoffmann
Department of Chemistry & Chemical Biology
Cornell University, Ithaca, NY 14853 (USA)
E-mail: rh34@cornell.edu
Dr. I. I. Naumov
Geophysical Laboratory, Carnegie Institution of Washington
5251 Broad Branch Rd. NW, Washington DC (USA)
Prof. R. J. Hemley
Department of Civil and Environmental Engineering
The George Washington University, Washington DC, 20052 (USA)
and
Lawrence Livermore National Laboratory
Livermore, CA 94550 (USA)
Supporting information and the ORCID identification number(s) for the author(s) of this article can be found under: http://dx.doi.org/10.1002/anie.201608490.

their own "attractors", and thus define regions of space associated with an ISQ.[16] The electron density within those regions may be integrated, leading to 1.45e in E^{II}, (approximately equal for both symmetry-distinct sites of this type; which is why from now on we will refer to both as E^{II}) and 0.65e, in E^{I}, respectively. Bader densities smaller than formal charges have been found previously.[17] We also calculated the Bader charges of LiF and MgO in the rock salt structure and found a charge of −0.87e on F, −1.74 on O. Thus even in highly ionic compounds the Bader basin densities only approach −1 and −2. We interpret the integrations obtained as indicating that in *Aba*2 Li at 60 GPa 2 electrons in ISQ E^{II}, 1 in E^{I}.

In a primitive cell that contains 20 Li atoms, we identify 8 E^{II} and 4 E^{I}. This Li phase can then be viewed as approximating an ionic crystal with the formula of $Li_{20}E^{II}{}_8E^{I}{}_4$, with each lithium providing one electron to the ISQs. This perspective is consistent with the electron localization function (ELF) analysis in previous work.[5] The question remains: if the orbitals of the 4 E sites in the primitive unit are singly occupied, why is *Aba*2 Li semiconducting instead of metallic or radical-like.

Figure 2a is another view of the structure. The ISQ E^{I} centers are clearly shown; they form pairs with a separation of only 1.3 Å. Such a small separation suggests an attractive interaction between the E^{I} ISQs. As we vary the pressure, the distances between atoms of course decrease on average. But as Figure 2b shows, while the Li–Li and Li–E^{I} distances decrease with increasing pressure, the short E^{I}–E^{I} (and Li–E^{II}) separation remains pretty constant. The E–E distance is a result of balancing several interactions including the E–E bonding energy and Li^{+} electrostatic energies.

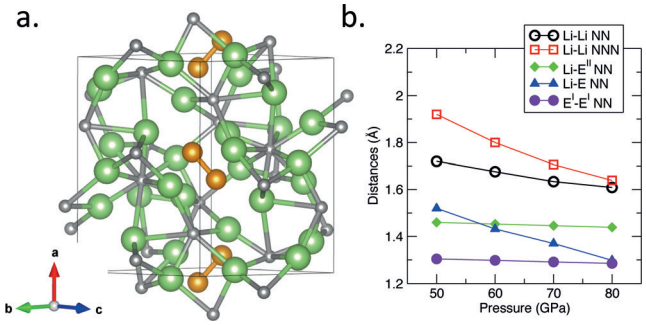

Figure 2. a) Li *Aba*2 structure showing the E ISQ pairs in cavities surrounded by Li atoms, the green and the golden balls show the positions of Li atoms and ISQs (E^{I} only); b) the inter-"atomic" distances as function of pressure.

We suspect there are E^{I}–E^{I} bonds in this material. Any bonding features can be investigated in real and in reciprocal space. The charge distribution in real space (Figure 1b) shows clearly the elevated electron population in the region between two neighboring E, consistent with population of a bonding orbital of the quasimolecule. Similar results can be seen from ELF (Supporting Information, Figure S1), band structure (Figure S2) and projected density of states (Figure S3).

The bonding character of levels can be examined by a crystal orbital Hamiltonian population (COHP) analysis, which characterizes the states in a given energy region with respect to their bonding or antibonding character between specified atoms.[18] A negative COHP indicates bonding; whereas positive COHP indicates antibonding (see the Methods section). With the help of the linear muffin-tin orbital (LMTO) method in an atomic sphere approximation (ASA), we could calculate COHPs in this system. We found significant negative COHP for neighboring E^{I}–E^{I} ISQs pairs below the Fermi level (Figure 3). For comparison, the COHP

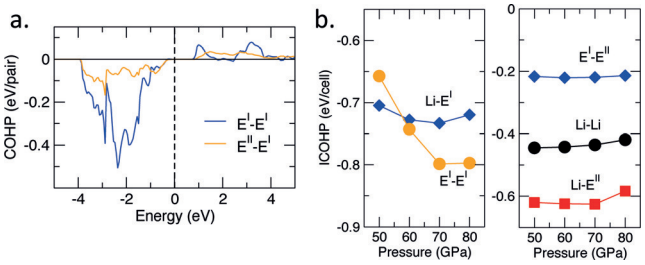

Figure 3. a) Crystal orbital Hamiltonian population (COHP) for pairs of ISQs in *Aba*2 Li at 60 GPa; b) integrated COHPs as a function of pressure.

between neighboring E^{II} and E^{I} ISQs (expected to be smaller, as the E^{II}–E^{I} distance is 1.9 Å, while E^{I}-E^{I} is 1.3 Å) is indeed substantially smaller. The COHP between two E^{II} ISQs (2.72 Å apart) is negligible. Figure 3 also shows significant ICOHP values for pairs of Li-ISQ and Li–Li. Their changes with pressure (Figure 3b) are not as large as those of E^{I}–E^{I}.

Importantly, the Fermi level of this phase, in the band gap, lies between the regions of negative and positive E^{I}–E^{I} COHPs. This is just what one would expect from a quasimolecular picture, bonding and antibonding states of the E^{I}–E^{I} ISQ pairs, split around the energy gap. The integrated COHP (ICOHP) can provide an estimate of the net strength of the bonding between a pair of species (atoms and ISQs). As shown in Figure 3b, this value is about −0.65 eV/pair at 50 GPa and decreases (stronger bonding) to about −0.8 at 70 and 80 GPa. Note (Figure 2) that the E^{I}–E^{I} distance is not changing much in this range. The ICOHP value indicates moderate bonding between the two E^{I} ISQs.

With these quasimolecules, we are in new territory for bonding, and need some calibration. For comparison, we calculated the ICOHP for two H atoms with the same distance of 1.3 Å as the E^{I}–E^{I} pair. The result is −2.65 eV per pair, substantially larger that the E^{I}–E^{I} value. It appears that insertion of centering nuclear charges enhances the chemical bonding. To this end, it is useful to examine directly the form of the bonding orbital between two E^{I} ISQs. We look for such orbitals through the associated Wannier functions. Using the Wannier90 program[19] in combination with ABINIT codes,[20] by iteration we found all (10) maximally localized WFs in *Aba*2-Li at 70 GPa, including two of them associated with the E^{I} ISQs at Wyckoff positions 2*a*. These WFs, centered between the two E^{I}, are shown in Figure 4 at different isosurfaces. One can see from the high isosurfaces that the

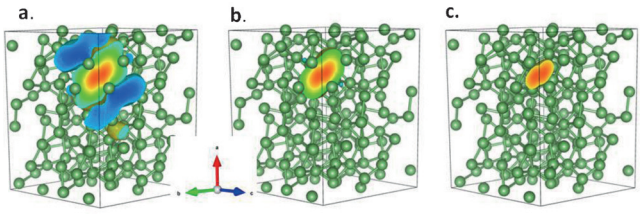

Figure 4. Maximally localized Wannier function with its center between two E^I SQs in *Aba*2 Li at 70 GPa. The results are shown in a 2×2×2 primitive unit cell for different isosurfaces: a) isosurface = ±0.25, b) ±1.00, c) ±2.50.

WF does resemble the bonding orbital between two E^I. Another perspective on these functions is to see them as being formed from s–p hybrids within a cluster of 4 Li atoms, two of them coming from one side and two from the other. This characterization reflects a subtle interconnection between the s–p electronic transition[21] and the development of interstitial charge in compressed Li. Note that the negative lobes of the WF (shown in blue) disappear for isosurfaces higher than ±1.0, and the spread of the function is 4.3 Å, which is approximately 3 times the E^I–E^I distance.

Looking for the orbital(s) responsible for bonding in another way, we plotted the band-decomposed charge densities (square of the wavefunctions) at the Γ point for the ten highest occupied bands. And in these we identified those having the largest projections on the E^I sites (Figure 5a,b). The first such state is two levels below the highest occupied state. The corresponding electron density is centered at a 2*a* Wyckoff position, but, as may be seen, is not aligned well with the E^I–E^I axis. However, there is one more state that should be taken into account, which is somewhat further down in energy (0.84 eV). This state has a density asymmetry that complements that of the state shown. The two states taken together produce a reasonably symmetrical E^I–E^I bond, as Figure 5c shows.

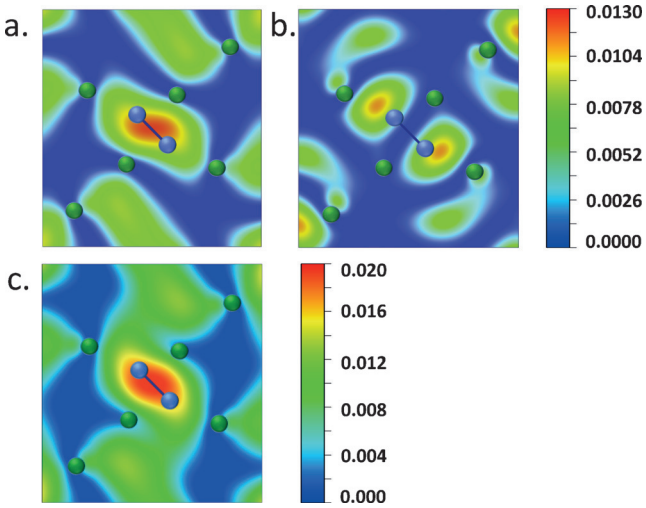

Figure 5. Electron densities computed for selected states of Aba2 Li at the *Γ* point at 60 GPa. a) Bonding state of an E^I–E^I pair (third state below highest occupied state at point); b) antibonding state of an E^I–E^I pair (sixth state above the lowest unoccupied state at point). c) Sum of the densities of orbital in (a), with a second orbital 0.84 eV below (see text).

In the bonding state, the electron density is maximized between the two ISQs, in accord with the absence of a node in the corresponding WF. In contrast, in the antibonding state, there is a node in the electron density between the E^I sites, and the associated WF is antisymmetric. Perhaps we can get another estimate of the bonding from the splitting in energy of the states primarily associated with the bonding. At the *Γ* point, the primary bonding state is 0.23 eV below the valence band maximum, while the antibonding one is 1.67 eV above. This provides an estimate of the splitting of the bonding and antibonding levels of an E^I–E^I quasimolecule of 2.67 eV at the point. At the same separation a stretched hydrogen molecule shows a splitting of 6.82 eV (at 1.3 Å, same distance as E^I–E^I), which gives us a rough calibration of the extent of interaction of ISQs in a quasimolecule. It is substantial, but less than the strong single bond in H_2.

An interesting question is why the two alkali metals, Li and Na, adopt different HPE structures at high pressures, even though they both contain one valence electron. At pressures above 200 GPa, Na adopts a double hexagonal close-packed (dhcp) structure, which we and others saw as analogous to a Ni_2In-type ionic structure, with 2 electrons occupying the ISQ in the structure.[3,22] Comparing with *Aba*2 Li, there is only one type of ISQ in dhcp Na, and it contains approximately 2 electrons. The major difference between Li and Na is that the former atom (and the corresponding cation) has a smaller radius; one would then expect relatively higher repulsive electrostatic energy among the Li^+ ions once the electrons are forced off them. We imagine that the creation of more ISQs with a lower charge state (−1 instead of −2) can more effectively separate/screen the Li ions and therefore reduce the Li^+–Li^+ repulsive energy.

Trying to get a computational handle on this idea, we optimized the geometry of Li in both *Aba*2 and dhcp structures at the same pressure, 60 GPa (with the HSE functional). In the dhcp structure, each Li^+ has 6 neighboring Li^+ ions with equal distance of 2.03 Å. In contrast, the distinct Li^+ ions in the *Aba*2 structure have 3, 4, and 5 neighboring Li^+ with interatomic distances less than 2.03 Å. Because more ISQs in *Aba*2 structure can better screen the Li^+ ions, the actual volume per Li is slightly lower for this structure (7.6 $Å^3$ for *Aba*2, and 7.8 $Å^3$ for dhcp). Though seeming small, this reduction of the volume gives the major contribution to the stabilization of Li *Aba*2 over the alternative dhcp structure. The enthalpy difference, $H = H^{Aba2} - H^{dhcp}$, is about −40 meV per Li; whereas the difference in the *PV* term, $PV = PV^{Aba2} - PV^{dhcp}$, is about −80 meV per Li.

In conclusion, in *Aba*2 Li at 80 GPa we find a short distance between pairs of ISQs containing approximately one electron. We show that this distance is clearly associated with the formation of bonding and antibonding quasimolecular states, like σ_g and σ_u^* of H_2, split across the gap in this phase. It is tempting to associate the semiconducting electronic nature of the material with quasimolecule formation.

Acknowledgements

The calculations were performed using NSF-funded XSEDE resources (TG-DMR130005), resources at the Centre for Scientific Computing supported by the CNSI, MRL, and NSF CNS-0960316, and Beijing CSRC computing resources. The work at Cornell and Carnegie was supported by EFree, an Energy Frontier Research Center funded by U.S. Department of Energy DOE), Office of Science, Office of Basic Energy Sciences under Award DE-SC0001057 and by CDAC, which is funded by the DOE/National Nuclear Security Administration under award DE-NA-0002006. Work at LLNL was performed under the auspices of DOE contract DE-AC52-07NA27344.

Keywords: density functional calculations · high pressure electrides · interstitial quasi-atoms · maximally localized Wannier functions · semiconducting lithium

How to cite: *Angew. Chem. Int. Ed.* **2017**, *56*, 972–975
Angew. Chem. **2017**, *129*, 992–995

[1] a) D. Issa, J. L. Dye, *J. Am. Chem. Soc.* **1982**, *104*, 3781–3782; b) R. H. Huang, M. K. Faber, K. J. Moeggenborg, D. L. Ward, J. L. Dye, *Nature* **1988**, *331*, 599–601; c) J. L. Dye, *Acc. Chem. Res.* **2009**, *42*, 1564–1572; d) D. J. Singh, H. Krakauer, C. Haas, W. E. Pickett, *Nature* **1993**, *365*, 39–42; e) K. Lee, S. W. Kim, Y. Toda, S. Matsuishi, H. Hosono, *Nature* **2013**, *494*, 336–340.
[2] T. Matsuoka, K. Shimizu, *Nature* **2009**, *458*, 186–189.
[3] Y. Ma, M. Eremets, A. R. Oganov, Y. Xie, I. Trojan, S. Medvedev, A. O. Lyakhov, M. Valle, V. Prakapenka, *Nature* **2009**, *458*, 182–183.
[4] a) H. L. Skriver, *Phys. Rev. Lett.* **1982**, *49*, 1768–1772; b) J. B. Neaton, N. W. Ashcroft, *Nature* **1999**, *400*, 141–144.
[5] M. Marques, M. I. McMahon, E. Gregoryanz, M. Hanfland, C. L. Guillaume, C. J. Pickard, G. J. Ackland, R. J. Nelmes, *Phys. Rev. Lett.* **2011**, *106*, 095502.
[6] J. A. Lv, Y. C. Wang, L. Zhu, Y. M. Ma, *Phys. Rev. Lett.* **2011**, *106*, 015503.
[7] P. F. Li, G. Y. Gao, Y. C. Wang, Y. M. Ma, *J. Phys. Chem. C* **2010**, *114*, 21745–21749.
[8] C. J. Pickard, R. J. Needs, *Nat. Mater.* **2010**, *9*, 624–627.
[9] a) M. Martinez-Canales, C. J. Pickard, R. J. Needs, *Phys. Rev. Lett.* **2012**, *108*, 045704; b) Q. Zhu, A. R. Oganov, A. O. Lyakhov, *Phys. Chem. Chem. Phys.* **2013**, *15*, 7696–7700; c) M.-s. Miao, X.-l. Wang, J. Brgoch, F. Spera, M. G. Jackson, G. Kresse, H.-q. Lin, *J. Am. Chem. Soc.* **2015**, *137*, 14122–14128; d) M. Marques, G. J. Ackland, L. F. Lundegaard, G. Stinton, R. J. Nelmes, M. I. McMahon, J. Contreras-Garcia, *Phys. Rev. Lett.* **2009**, *103*, 115501.
[10] M. S. Miao, R. Hoffmann, *Acc. Chem. Res.* **2014**, *47*, 1311–1317.
[11] M.-S. Miao, R. Hoffmann, *J. Am. Chem. Soc.* **2015**, *137*, 3631–3637.
[12] J. P. Perdew, K. Burke, M. Ernzerhof, *Phys. Rev. Lett.* **1996**, *77*, 3865–3868.
[13] G. Kresse, D. Joubert, *Phys. Rev. B* **1999**, *59*, 1758–1775.
[14] G. Kresse, J. Furthmuller, *Phys. Rev. B* **1996**, *54*, 11169–11186.
[15] R. Bader, *Atoms in Molecules: A Quantum Theory*, Oxford University Press, Oxford, **1990**.
[16] a) W. L. Cao, C. Gatti, P. J. Macdougall, R. F. W. Bader, *Chem. Phys. Lett.* **1987**, *141*, 380–385; H. Mizoguchi, M. Okunaka, M. Kitano, S. Matsuishi, T. Yokoyama, H. Hosono, *Inorg. Chem.* **2016**, *55*, 8833–8838.
[17] a) G. K. H. Madsen, C. Gatti, B. B. Iversen, Lj. Damjanovic, G. D. Stucky, V. I. Srdanov, *Phys. Rev. B* **1999**, *59*, 12359–12369; W. Bronger, A. Baranov, F. R. Wagner, R. Kniep, *Z. Anorg. Allg. Chem.* **2007**, *633*, 2553–2557; A. Baranov, M. Kohout, F. R. Wagner, Y. Grin, R. Kniep, W. Bronger, *Z. Anorg. Allg. Chem.* **2008**, *634*, 2747–2753; A. Ormeci, A. Simon, Y. Grin, *Angew. Chem. Int. Ed.* **2010**, *49*, 8997–9001; *Angew. Chem.* **2010**, *122*, 9182–9186.
[18] R. Dronskowski, P. E. Blochl, *J. Phys. Chem.* **1993**, *97*, 8617–8624.
[19] A. A. Mostofi, J. R. Yates, Y.-S. Lee, I. Souza, D. Vanderbilt, N. Marzari, *Comput. Phys. Commun.* **2008**, *178*, 685–699.
[20] X. Gonze, J. M. Beuken, R. Caracas, F. Detraux, M. Fuchs, G. M. Rignanese, L. Sindic, M. Verstraete, G. Zerah, F. Jollet, M. Torrent, A. Roy, M. Mikami, P. Ghosez, J. Y. Raty, D. C. Allan, *Comput. Mater. Sci.* **2002**, *25*, 478–492.
[21] I. I. Naumov, R. J. Hemley, *Phys. Rev. Lett.* **2015**, *114*, 156403.
[22] a) M. Marques, M. Santoro, C. L. Guillaume, F. A. Gorelli, J. Contreras-Garcia, R. T. Howie, A. F. Goncharov, E. Gregoryanz, *Phys. Rev. B* **2011**, *83*, 184106; b) M. Gatti, I. V. Tokatly, A. Rubio, *Phys. Rev. Lett.* **2010**, *104*, 216404.

Manuscript received: August 30, 2016
Revised: October 29, 2016
Final Article published: December 21, 2016

